

PRELIMINARY RESULTS OF AN ELECTRIC VEHICLE TRACTION SYSTEM PROTOTYPE BASED ON FUEL-CELL AND SWITCHED RELUCTANCE MOTOR – GENERATOR

Pedro Pereira de Paula¹
Wanderlei Marinho da Silva²

Universidade Cruzeiro do Sul – UNICSUL
São Paulo – SP – Brasil
¹ppdepaula@uol.com.br
²wmarinho@usp.br

Gilberto Janólio³
Angelo Massatoshi Ebesui³
Gerhard Ett³
Volkmar Ett³

Grupo Electrocell
São Paulo – SP – Brasil
³electrocel@electrocell.com.br

Abstract – This paper shows some aspects of the development of a fuel cell based propulsion system prototype for electric vehicles and some preliminary results. A switched reluctance motor/generator – SRM/G - with 3 phases, 6 stator poles and 4 rotor poles is connected to the DC link bus through an asymmetric half-bridge converter which is fed by a PEM (Proton Exchange Membrane) fuel cell. The control functions of this drive are performed by an 8-bit microcontroller. This system is designed to allow the studies of the motoring, generating and regenerative braking operations aiming the development of the necessary knowledge to design propulsion systems for several kinds of vehicles. Some simulations and tests results are also presented.

I INTRODUCTION

Nowadays the mankind has found a lot of reasons to try to develop propulsion systems achieving the requirements of a minimum pollution emissions and the fuel cell arises as an attractive alternative. The idea of moving vehicles expelling a water stream seems like a dream from an environmental point of view. There is a lot of work to do before this idea becomes a reality and this paper brings a contribution to this dream.

This paper aims the description of the development of a test bench based on fuel cell and switched reluctance motor and generator designed to study the capabilities of this kind of system applied to the propulsion of electric vehicles. This system prototype comprises a PEM (Proton Exchange Membrane) fuel cell and a switched reluctance motor-generator connected to the DC link bus through an asymmetric half-bridge converter.

Among the reasons to use the fuel cell as a source of electrical energy, two of them stands out: a) the energy of a fuel cell is derived from hydrogen, which is extracted from a great number of renewable resources; b) the conversion of energy has no emissions. These features puts the fuel cell as a viable energy source for the future in many applications in the automotive, commercial, residential and portable areas.

The switched reluctance machine combines a rugged brushless construction, high reliability and a very good performance on a wide speed range. Taking into account suitable design and control considerations, the switched reluctance machines have demonstrated a good

performance from a few watts up to hundreds of kilowatts. This fact contributes to consider this machine as a serious candidate to this application.

The four quadrant performance is achieved with a single power electronic converter allowing the motor, generator and regenerative braking operations. A suitable control strategy is enough to fulfill the four quadrant operation requirements.

The efficiency, torque, torque ripple, noise, power-weight ratio and power density are the main characteristics of an electric propulsion system that should be properly weighted to analyze its suitability to a particular application. This test bench offers the possibility of getting several conclusions about this kind of system.

The components of this system are already manufactured and the individual tests are in the beginning. After the completion of these tests the full system will be assembled to study its features as a whole.

II THE SWITCHED RELUCTANCE MACHINE

The switched reluctance machine is basically a doubly salient structure in which concentric coils are mounted around the stator poles and the rotors have neither windings nor permanent magnets. The stator and the rotor are assembled with ferromagnetic laminations. The coils of opposite stator coils are connected in series or in parallel with convenient polarities to create, when electric current flows in them, the N and S pole pairs of a phase. The cross-section of the machine is shown in Fig. 9.

The motor has an interior rotor and it moves always in a direction in which the self-inductance of the excited coil is increased. In a good design, the mutual inductance between phases is nearly zero and the reluctance torque is the only one developed by this motor.

Since the torque is developed due to the tendency of alignment of the rotor pole axis with the axis of excited coils, the polarity of the current in the coil, during the conduction period of the power switches makes no difference. This fact contributes to a simplification of the converter scheme, since it is not necessary to change the sense of the current [1-4].

Fig. 1 shows the converter scheme used in this work which permits four quadrant operations of the drive. In this scheme the phases are independent from each other and if

a failure in one phase occurs, the machine may continue the operation within a limited power range.

The converter is of the asymmetric half-bridge type. Having in mind the nature of torque production one may conclude that it is necessary to establish the electric current in each coil, sequentially, with the switching control signals derived from the angular position sensor.

There are 2 operation modes for this prototype converter: the single-pulse voltage and the chopping-voltage. In the chopping-voltage mode, at the beginning of the conduction period of one phase, e.g., phase 1, the switches Q1 and Q2 are turned on and the current flows through the switches and phase 1. During this period, by using a reference value and a current feedback, the current value is maintained below the maximum by turning on and off one of these switches, e.g., Q1. When Q1 is turned off the current flows through the phase, Q2 and D2. At the end of the conduction period both switches are turned off and the current flows through the phase and the freewheeling diodes returning to the supply. Pulse width modulation (PWM) is suitable for controlling the current and this operation mode is used for low and medium speeds [5-7].

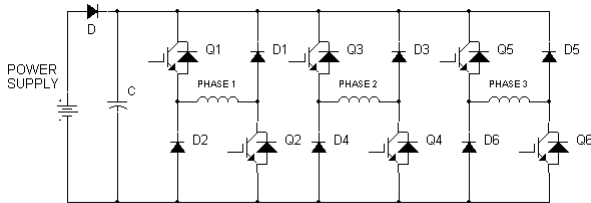


Fig. 1 - Asymmetric half-bridge converter

As the speed increases, the time required for the rotor to travel an angle equivalent to the conduction angle of the power switches becomes smaller. Above the so-called base speed the conduction time will be such that the current is switched on and off only once in each conduction period. Then we have the so-called voltage-fed or single-pulse mode [1-2].

The regenerative braking or generator operation presented in this paper regards the single-pulse operating mode and is achieved through a suitable delay in the conduction angles of power switches of the phases. This kind of generator has been studied for applications where a wide speed range, robustness and fault tolerance are the main requirements to achieve. The generator supplies the DC link through the same converter used for the motor operation and a suitable angle and speed control is necessary to establish this operation [2, 8-10].

The generator presented in this paper is self-excited. During the conduction period of the power switches, it draws energy from the DC link and this is the excitation period. At the end of this period, both power switches are turned off and the current flows to DC link through the diodes and this is the generating period. The generating current is sustained while the rotor displacement causes a variation in the phase inductance. The generating current is shared between the next phase to be excited, the bus capacitor and the load. The angles mentioned may be adjusted properly to optimize the operation of the drive [1-2].

III SIMULATIONS

A. Finite-Element Analysis

The first step towards the design aiming the gross dimensions of machine is the usage of the classical equations. These equations are related to the torque, electric loading and magnetic loading. These parameters are calculated by using guide values of torque per unit rotor volume, air gap shear stress, output coefficient, current densities in the conductors, etc. Having in mind the resources available and related constraints, this first step gives an outline of the machine [1,6].

After this step is given, one must choose a way to get a refinement of the solution aiming the final dimensions and other important characteristics of the machine, like materials choice, manufacturing processes, etc. This way may be a combination of usage of classical analytical methods and computer methods. Another aspect to be considered is the development of a large amount of experimental work and prototypes manufacturing. Naturally, these activities related to the prototypes could be a serious inconvenient in order to developing new equipment at competitive prices. Nowadays one may notice that modern computer methods are reaching an accuracy and a reliability that precludes a lot of working time with the manufacturing and testing of prototypes[2].

These activities reported in this paper were developed using the computer software FLUX2D[11] that solves complex electromagnetic field problems by using the finite-element method. The solution of bi-dimensional problems is obtained by the discretization of the motor cross section in a great number of small elements of area called finite elements, as shown in Fig. 2. This software considers the non-linearity of the domain of study and solves the partial differential equations to get each nodal value of the vector potential A . After that all the field quantities such as magnetic flux, magnetic induction and so on can be determined.

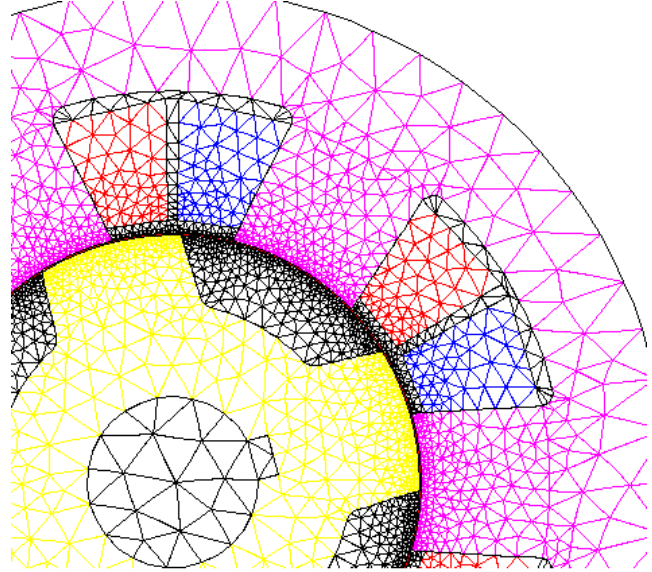


Fig. 2 - Mesh

Our domain of study is the machine cross section, which corresponds to a bi-dimensional model. An automatic mesh generator is available in this software. It

allows also a greater refinement of the mesh where the user expects a higher degree of changing of the magnetic quantities. To get a homogeneous mesh, the mesh is refined with a sub-routine that uses the Delaunay's method. This method aims to make each element of area of the discretized domain, as much as possible, as an equilateral triangle.

The cross section studied is split up into regions characterized by the different materials used in the construction of the several components of the motor, e.g. the shaft, the rotor laminations, the stator laminations, the conductors, the air-gap, etc. Each material is characterized by its physical properties. Some of these regions can be split up still further as a matter of convenience of design or mesh generation. All the materials are considered to have isotropic physical properties.

The domain discretization contains 9926 triangular elements. The greater refinement of the mesh is around the air-gap, where a ring with a small thickness is positioned. This ring defines a region assigned as a rotating air-gap. This is a characteristic available in the software FLUX2D intended to study the cases which have a relative movement between some regions. This rotating air-gap is a surface with a single layer of elements and is positioned between the rotor and the stator. This rotating air-gap allows an improvement of the solution of problems with moving parts because it keeps the number of equations to be solved and also keeps the mesh.

To solve the field problems of our model, we have been imposing the Dirichlet condition in the nodes pertaining to the external circumference of the stator laminations. It means that no one line of magnetic flux crosses this circumference, or the vector potentials \mathbf{A} are null in these nodes.

Having obtained the solution of the field problem, the software post-processing stage allows the generation of several outputs: flux plots, flux calculations, flux density contours, graphics of magnetic induction variation, magnetic induction vector plot, force and torque, self and mutual inductance and some other quantities of interest. In this software there are two kinds of post-processing routines: a numerical one that allows the numeric treatment of the resulting quantities, and a graphical one that provides a visualization of the resulting quantities.

B. Mathcad Simulation

The steady state performance simulation in this paper is achieved using a Mathcad environment. It is assumed that the mutual inductances between phases are negligible. This simulation is being developed and allows the calculation of the instantaneous phase current and flux linkage and it also derives the flux linkage versus phase current for the single-pulse mode. Further developments will allow the calculation of the instantaneous torque. Although it is recognized that the mutual inductance influences the performance[2,10,12], this kind of approach allows a fast method to get useful results.

When both power switches are turned on, the DC bus voltage, V_{DC} , is applied to the phase winding and the voltage equation is:

$$V_{DC} = R \cdot i + \frac{d\Psi}{dt} \quad (01)$$

where, R is the phase resistance, i is the instantaneous current and Ψ is the flux linkage.

The flux linkage is calculated, considering constant angular speed ω , according to equation (02);

$$\Psi = \frac{1}{\omega} \int_{\theta_0}^{\theta_c} (V_{DC} - R \cdot i) d\theta + \Psi_0 \quad (02)$$

where θ_0 is the turn on angle and θ_c is the angle at which the power switches are opened. During this conduction period, once the flux linkage is known the instantaneous current can be calculated from the magnetization curves of the machine in a step-by-step manner [1]. After θ_c the current flows through the diodes and the phase winding and the sign of the voltage applied to the phase changes. During this period, the instantaneous current can be calculated following a similar method.

IV THE PEM FUEL CELL PROTOTYPE

The fuel cell is a electrochemical device that produces electrical energy from a chemical reaction and without combustion. Hence this device does not delivery pollutants to the environment. The fuel cell basically has an electrolyte layer in contact with porous anode and cathode on either side as depicted in Fig. 3. The hydrogen rich fuel and oxidant gases flow through the anode and cathode, respectively, into the electrolyte and generate electrical energy by the electrochemical oxidation of fuel and the electrochemical reduction of oxygen.

The fuel cell type of this prototype system is a proton exchange membrane (PEM) that has the advantage of operating in a relatively low temperature (about 80 °C), high power density (about 330 W/kg) and the capability of rapid response to the power demand changes. This prototype fuel cell is fed from hydrogen and oxygen containers. The flow of these gases are adjusted properly to match the power demand of the system.

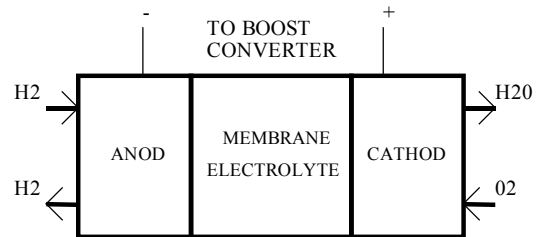


Fig. 3 - Schematic drawing of a PEM Fuel Cell

The polarization curve of the fuel cell unity is shown in Fig. 4. During the full load operation the current density of each unity is 0.5 A/cm² and a e.m.f. of 0.6 V is generated between terminals. This fuel cell stack has 40 unities in series, a surface of 100 cm² and the capability of supplying 1200 W in a 24 V DC bus. A boost converter is connected to the output of the fuel cell to rise the voltage level to the 250 V required by the switched reluctance machine.

Fig. 5 shows the fuel cell stack and Fig. 6 shows the fuel cell apparatus that comprises the stack, the cooling system, monitoring instruments and a PLC to perform the control functions.

V POWER AND CONTROL SYSTEM

The first aspect to highlight is that this is an experimental system designed to study the characteristics of this kind of equipment and aiming the development of the control algorithms. For the purposes of this work suitable control flexibility is achieved with 8 bit microcontroller.

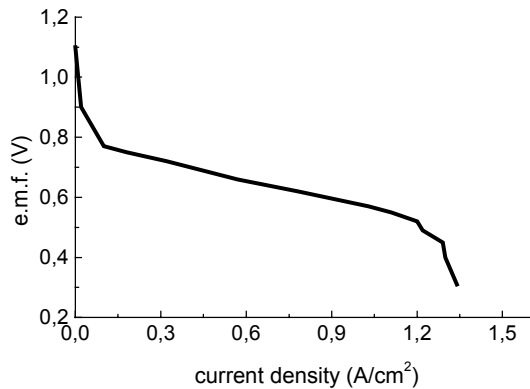


Fig. 4 – Polarization curve

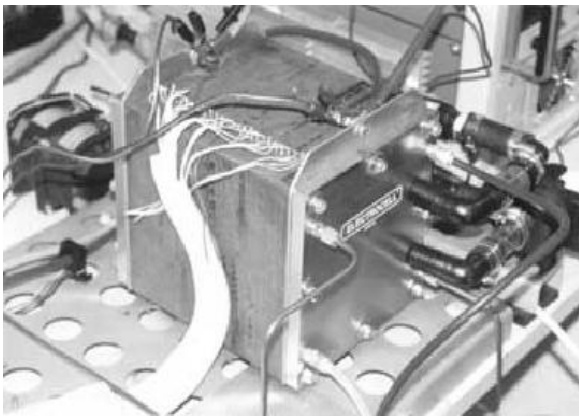


Fig. 5 – Fuel cell stack



Fig. 6 – Fuel cell apparatus

The complete system is depicted in Fig. 7. One can notice that for the purpose of these studies, a boost converter is necessary to match the low voltage level of the fuel cell to the voltage level of the motor/generator machine. The boost converter must be sized on the full power of the Fuel Cell stack.

The diode at the output of the fuel cell stack is necessary to prevent the negative current going into the stack. Due to the negative current, it is possible that the cell reversal could occur and damage the fuel cell stack. The ripple current seen by the fuel cell stack due to the switching of the boost converter has to be low. The power drawn from the fuel cell is controlled by controlling the output current of the DC/DC converter.

The issues to be considered in the system integration are [13]:

- system dc voltage: the optimum dc voltage with and without the DC/DC converter;
- rate of increase of the output power of the fuel cell stack;
- shutting-off the entire system;
- coordination between subsystems for optimum operation;
- electro-magnetic interference and noise in the electrical signals;
- ground loop, grounding, and ground faults;
- leakage current limitations to meet the safety requirements;
- isolation of the fuel cell stack from the drive system;
- charging the capacitors of the inverter and technology of capacitors in the dc side;
- effect on the fuel input if the load is suddenly disconnected;
- amount of regeneration allowed (regeneration is the process of feeding the kinetic energy in the motor to the DC link);
- coordination between regenerative braking and mechanical braking;
- management of the regenerative energy;
- matching the fuel cell output characteristics with the characteristics of the drive system;
- advanced sensors for fuel flow measurement, temperature/pressure regulation, and for sensing the various chemical reactions in the fuel cell unit.

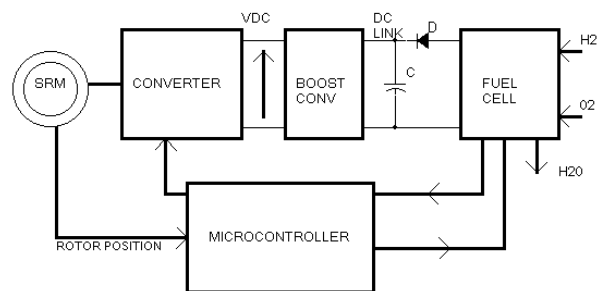


Fig. 7 – Drive system structure and the fuel cell.

For the purposes of this work suitable control flexibility is achieved with the PIC16C73 microcontroller from Microchip. The PIC16C73 IC perform several functions:

- decoding of rotor position sensors;
- advance angle control;
- speed control;
- dynamic braking;
- current limiting;
- hard, soft-switching and single-pulse operation.

By controlling the upper and lower transistors switching times independently, this feature allows the operation in the single-pulse mode and in the PWM mode. The former mode means that both power switches of each phase are turned on and off only once during the conduction period defined by the rotor angular position sensor. The latter mode provides the control of the average value of the applied voltage by using the pulse-width modulation (PWM). The controller allows the implementation of two modes of chopping the supply voltage: the hard chopping and the soft chopping. The signals of the rotor angular position are derived from optical sensors. The next step of this work is the development of indirect rotor position detection schemes.

VI RESULTS

A. Features of the machine

Fig. 8 shows the machine and the power converter. The machine prototype has 3 phases, 6 stator poles and 4 rotor poles and is designed to develop 3.8 N.m until 3000 rpm and to operate under constant power of 1200 W from 3000 rpm to 10000 rpm. The nominal voltage of the DC link is 250 V. In the lower speed range, the maximum current will be limited by chopping-voltage (PWM) and in the upper speed range the machine will operate in the single-pulse operating mode. The machine frame is cradled to allow the measurement of the average torque during the steady state operation and the measurement of the static torque versus rotor position for several current values. Each stator pole has one main winding and a search coil with few thin wire turns with their outputs accessible. This feature allows the implementation of several power converter schemes and allows the measurements of the flux linkages on-line. The machine prototype has two end-shafts, one for coupling the mechanical load and the other for coupling an optical rotor position sensor and one encoder. The search coils and the encoder will support the developments of the indirect rotor position schemes.

The nominal power of the power converter is 10 kW and the DC link bus voltage is 250 V. The design of this converter allows the implementation of several schemes to supply electric power to switched reluctance motors and generators and the power switches are IGBT's.

B. Finite-element method results

The assembling of the full system prototype is being completed and the equipment will be ready for tests very soon. The simulations are being developed to study the integration of the electric machine and its converter with the fuel cell.

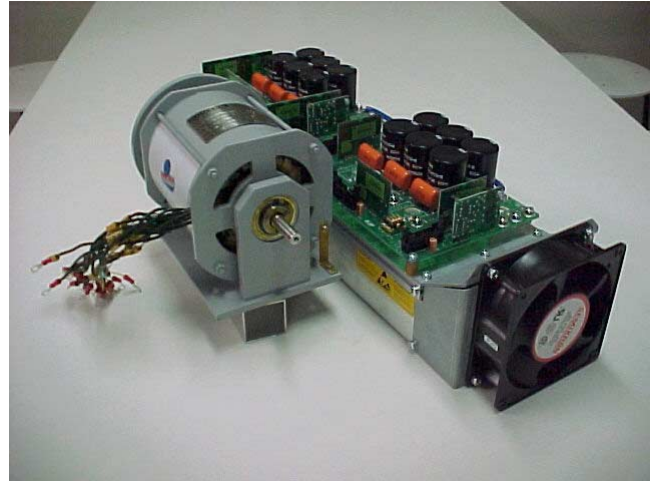


Fig. 8 – Machine and power converter

In this kind of machine design, the magnetostatic finite-element analysis brings useful results and the next figures are included to illustrate this approach. Fig. 9 shows the flux plot obtained for one rotor position with constant current flowing in one phase. A lot of calculations of this kind for several rotor positions and several current values are conducted to obtain the magnetization curves of the machine, as shown in Fig. 10. This figure shows only five magnetization curves for five rotor positions.

The post-processing stage of the software FLUX2D allows also the calculation of the self-inductance of the phase winding as a function of rotor position and current, as displayed in Fig. 11. The inductance keeps its minimum value while there is no superposition of the rotor and stator poles and in this range of rotor displacement the current does not affect this value. Continuing the displacement of the rotor poles, after the beginning of the superposition with the stator poles, the self-inductance values grows and reaches its maximum value when the rotor pole axis aligns the stator pole axis of the phase. In this displacement range a strong influence of the current (or saturation of the magnetic materials) occurs.

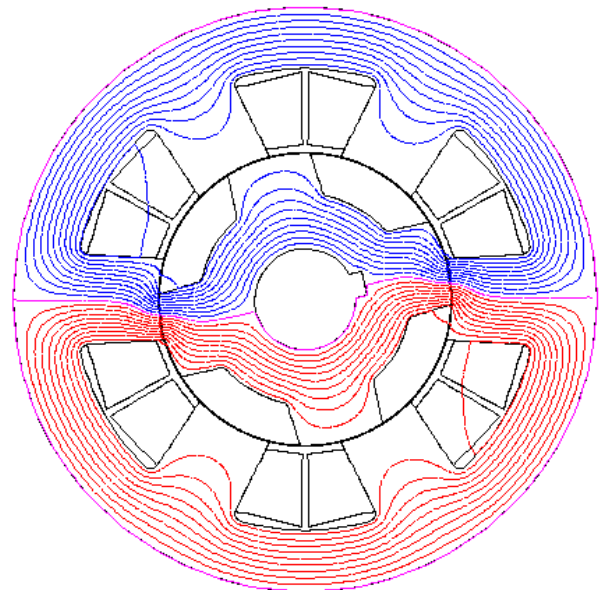


Fig. 9 – Flux plot

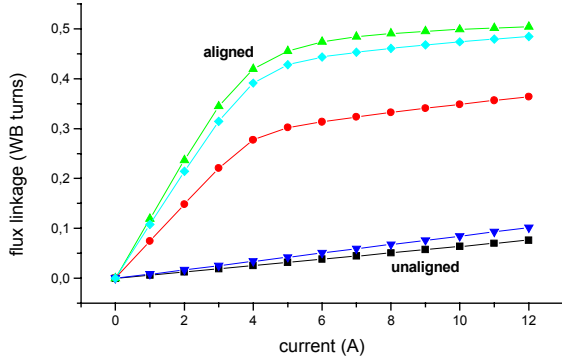


Fig. 10 – Magnetization curves

To minimize the VA requirements of the power converter, the machine should experience a strong saturation [4]. On the other hand, this saturation should occur mainly in the stator and rotor poles to minimize the core losses. This software is an useful tool to design the geometry of the poles and yokes to achieve these requirements.

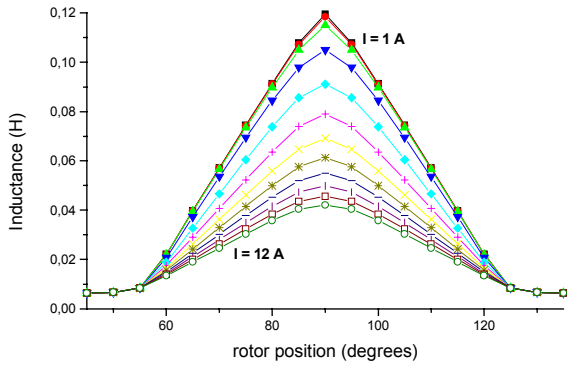


Fig. 11 – Self-inductance versus rotor position

Fig. 12 displays the static torque as a function of rotor position for 12 values of phase current. One may notice while approaching the alignment rotor position the torque decreases due to the saturation of the stator and rotor poles. The torque is not zero before the beginning of the superposition of the rotor and stator poles due to the fringing flux effects.

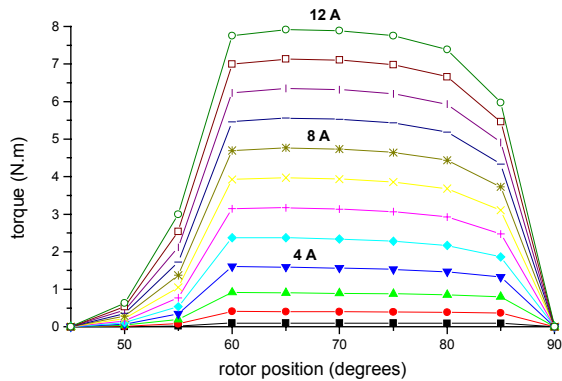


Fig. 12 – Static torque

From the results showed in Fig. 10 it is possible to assess the capability of the chosen design to developing the required average torque, as depicted in Fig. 13, and assuming the feasibility of imposing ideal rectangular current waveforms. Suppose that, observing Fig. 10, when the rotor pole axis position is at 45 degrees before alignment ($\theta_{on} = 45$), the power switches are turned on and the current reaches instantaneously some chosen value in the range of the horizontal axis. During the rotor displacement, the current is constant and maintained until the rotor axis reaches the alignment position, when the power switches are turned off and the current changes instantaneously to zero, corresponding to a conduction angle of 45 degrees ($\theta_c = 45$) and a turn off angle of 90 degrees ($\theta_{off} = 90$). The operating point, on the set of magnetization curves, follows a trajectory, in the counterclockwise sense, limited by the lower curve of Fig. 10, a vertical straight line which crosses the horizontal axis at the chosen maximum current value and the upper curve of Fig. 10.

The area encircled by this trajectory corresponds to the energy converted to mechanical energy by phase cycle [1,2], W , and the average torque is derived from equation (03), where m is the number of phases and N_r is the number of rotor poles:

$$T_{avg} = \frac{m \cdot N_r \cdot W}{2\pi} \quad (03)$$

This procedure gives the upper curve of Fig. 13. Similarly, two another curves are obtained for conduction angles of 30 degrees for $\theta_{on} = 45$ and $\theta_{on} = 55$. These curves shows the fundamental importance of the implementation of a suitable control strategy to optimize the performance of this kind of machine, since a proper delay of the turn on angle increases the torque.

C. Mathcad results

The magnetostatic simulations conducted with FLUX2D were made in steps of 5 degrees, from 45 degrees (unaligned rotor position) to 90 degrees (rotor pole axis alignment with stator pole axis of the excited phase). The current values span from 1 to 12 A in steps of 1 A. These simulations result in a set of 10 magnetization curves of the flux linkage versus current for 10 rotor positions. This set of curves is used by the Mathcad simulation for the interpolation of a $\psi \times \theta \times i$ surface shown in Fig. 14. For each step of the simulation, from the flux linkage value calculated with equation (02) for the actual rotor position θ , the instantaneous current value of the phase current is obtained by interpolation on this surface. Following this procedure, the instantaneous values of phase current and flux linkage are calculated as shown in Fig. 15 and 16. From these values, the flux linkage versus current for one cycle is depicted as in Fig. 17. These figures were obtained for the DC link voltage set in 250 V, the rotor speed is 3000 rpm, the conduction of the power switches begins 40.5 degrees before the alignment and the conduction angle is 30 degrees.

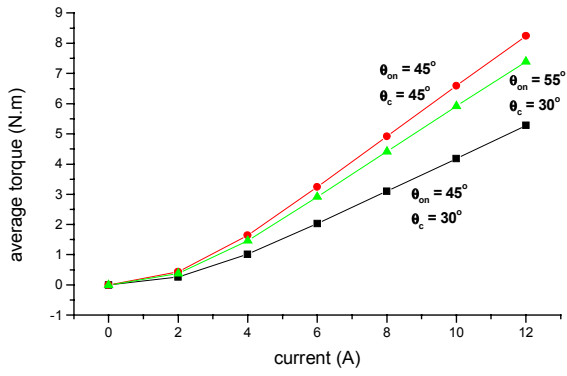


Fig. 13 – Average torque

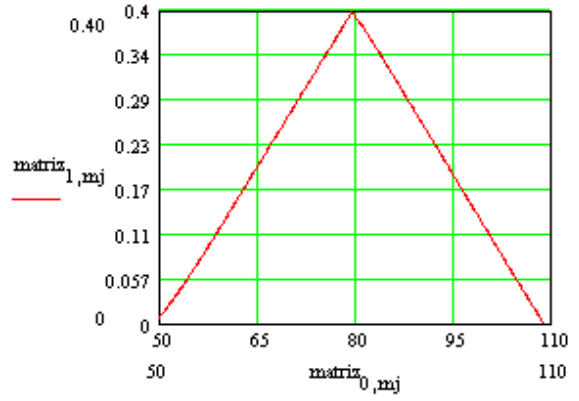


Fig. 16 – Flux linkage x time

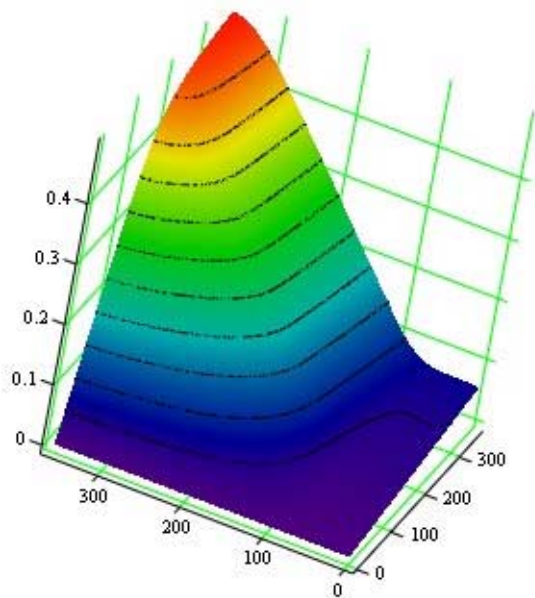


Fig. 14 – Surface $\psi \times \theta \times i$

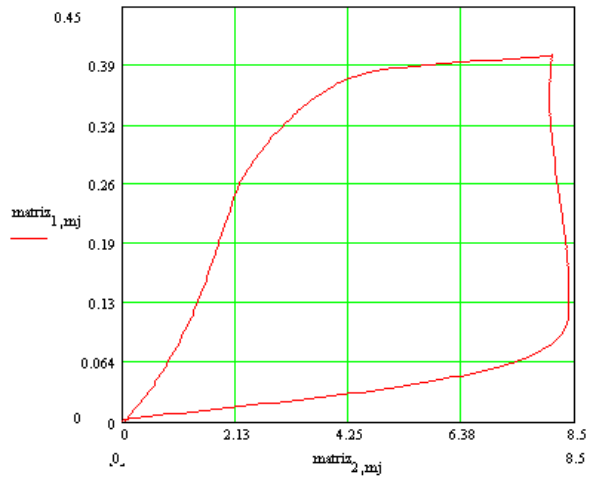


Fig. 17 – Flux linkage x phase current

D. Preliminary tests results

Next two figures are included as illustrations of the preliminary tests results. This kind of electric machine operates in a succession of electrical transients and the correct choice of the control parameters is very important to achieve the four quadrants operation requirements. The preliminary tests were made without load aiming an assessment of control parameters.

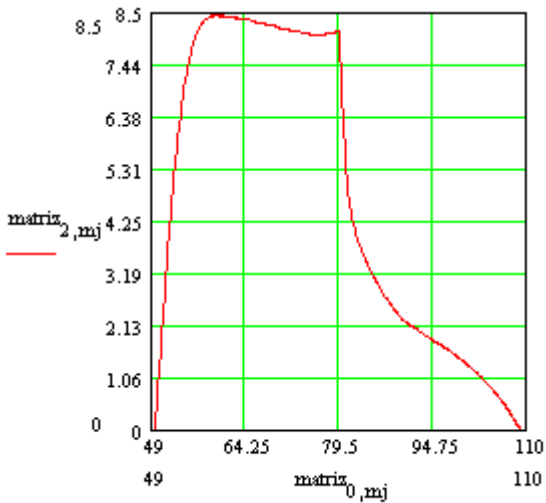


Fig. 15 – Phase current x time

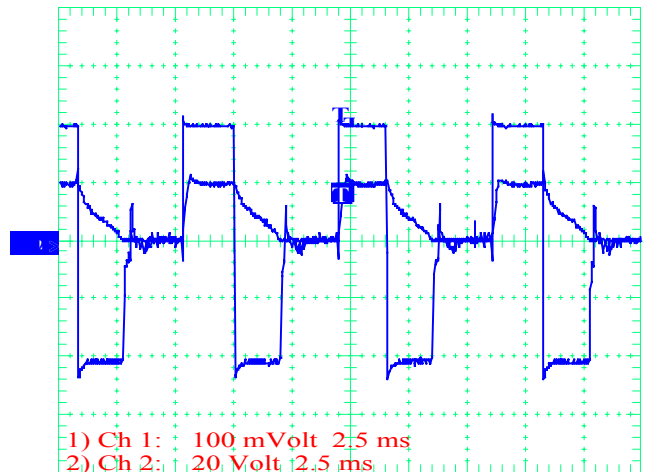


Fig. 18 – Phase voltage(Ch 2) and current(ch 1), no-load

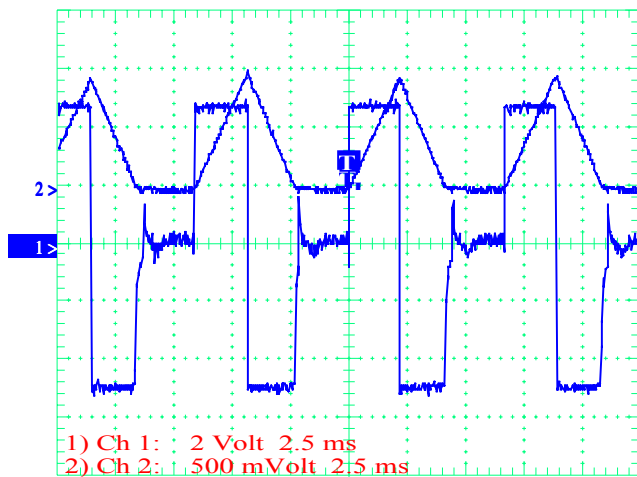


Fig. 19 – Search coil : e.m.f (Ch 1); flux linkage (Ch 2)

Figures 18 and 19 show some tests results when the motor is fed in the single pulse operation mode, with the DC link voltage adjusted at 40 volts and the rotor speed is constant and equal to 2250 rpm. The power switches are turned on and off in a fixed frequency, controlled by the rotor position feedback signals. In this operation mode the conduction period is such that the phase current is switched on and off only once per cycle. Fig. 18 shows the current and voltage waveform of one phase and Fig 19 shows the e.m.f. and the flux linkage of the search coil mounted in the same stator poles of this phase.

VII CONCLUSIONS

This paper shows some design aspects of an application of the switched reluctance motor/generator in a propulsion system prototype for electric vehicles having a fuel cell as a primary energy source. The assembling of the whole system is being completed and, by now, only some preliminary tests results of the components are available.

The usage of the finite-element method and Mathcad simulations as tools to the design are focused, which have been proved well. Further developments of the Mathcad simulations of this machine will calculate the instantaneous electromagnetic torque. For the upper speed range, the torque ripple is not a problem, but in the lower speed range it can impact the propulsion system performance. This problem can be treated with suitable design choices and by current profile. As an illustration, Fig. 20 is included, to show the torque calculated with the finite-element method coupled with circuit equations for another machine [2,12,14], for unfavourable set of control parameters. The FEM approach takes into account the whole machine, including the mutual inductances, has a better precision but has the disadvantage of taking a lot of computation time. The Mathcad approach takes less time due to the assumption that all phases have the same performance and the mutual effects are negligible.

The types of motors mainly considered for electric vehicles applications are: three phase induction motor, permanent magnet machines and the switched reluctance motor. Among these three options, we decided to develop this prototype system with a switched reluctance machine. Further developments of these activities will show the

advantages and disadvantages of using this kind of machine in this application.

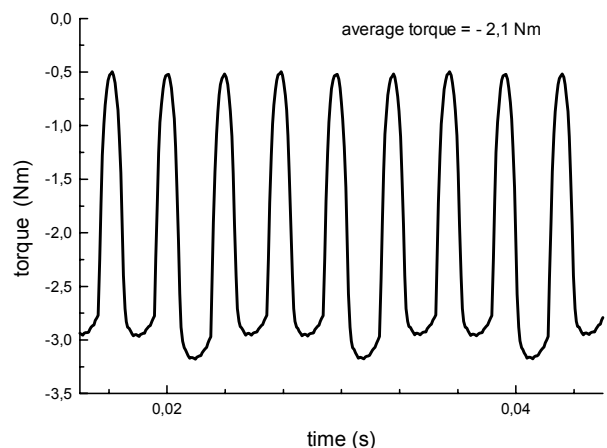


Fig.20 - Torque waveform, single-pulse, motor simulation

VIII ACKNOWLEDGEMENTS

The authors acknowledges the students at UNICSUL and Mr. Luciano Benitez Pereira who have been working in these activities. Thanks are also due to the company GLOBALMAG for the fluxmeter used in the measurements of the flux linkages.

IX REFERENCES

- [1] T.J.E. Miller. *Switched Reluctance Motors and their Control*. Oxford, Magna Physics Pub., 1993.
- [2] P.P. de Paula, *Aspects of design, simulation and operation of switched reluctance generators and motors*, Ph.D. Thesis (In Portuguese). EPUSP, São Paulo. 2000.
- [3] P.J Lawrenson et al, "Switched-speed switched reluctance motors", in *IEEE Proc.*, v.127, Pt.B, n.4, jul.1980.
- [4] T.J.E Miller, "Converter volt-ampere requirements of the SRM drive", in *Proc. of IEEE-IAS Annual Meeting*, s.l., oct.1984.
- [5] W.M. da Silva, L.C.C. de Araújo and P.P. de Paula, "A SRM drive design with dedicated drive and control circuits including experimental results", in *Proc. Conf. Power Conversion and Intelligent Motion - PCIM'99*, Chicago, USA, November 1999.
- [6] P.P. de Paula. *Design and Analysis of a SRM by Using the Finite-Element Method*. MSc Dissertation. EPUSP, São Paulo, 1993.
- [7] W M Silva, S I Nabeta, P P de Paula. "Low Power Switched Reluctance Generator Drive System Operation and Control" Drive System Operation and Control. INDUSCON-2000 IEEE Industry Applications Conference- Porto Alegre – RS – Brazil, 2000.
- [8] A.V. Radun, "Generating with the switched reluctance motor", in *Proceedings of APEC'94*, 1994, pp.41-46.
- [9] T. Sawata, P.C. Kjaer, C. Cossar and T.J.E. Miller, "A control strategy for the switched reluctance generator", in *Proceedings of ICM'98*, 1998, vol.3, pp.2131-2136.
- [10] R. Inderka, M. Menne and R.W. De Doncker, "Generator operation of a switched reluctance machine drive for electric vehicles", in *Proceedings of EPE99 (CD)*, 1999.
- [11] Laboratoire d'Electrotechnique de Grenoble, *FLUX2D: logiciel de calcul électromagnétique par éléments finis*, LEG-CEDRAT.
- [12] P.P. de Paula, W.M. da Silva, S.I. Nabeta and J.R. Cardoso, "Modelling a switched reluctance motor/generator by using the finite-element method coupled with circuit equations", in *Proceedings of the International Conference on Electrical Machines – ICM 2000*, Helsinki, Finland, pp.1752-1756.
- [13] K. Rajashekara, "Propulsion System Issues in Electric and Hybrid Vehicles," International Power Electronics Conference, 1995.
- [14] P.P. de Paula, W.M. da Silva, S.I. Nabeta and J.R. Cardoso, "Simulation of a switched reluctance motor/generator by using the finite-element method coupled with circuit equations", in *Revista Ciência & Engenharia*, ano 9, n 2, jul/dez 2000, pp. 28-33, Uberlândia, MG, Brasil, ISSN 0103-944X.